

pubs.acs.org/JPCA Article

# Trend in the Electron Affinities of Fluorophenyl Radicals $\cdot C_6H_{5-x}F_x$ (1 $\leq x \leq 4$ )

Conor J. McGee, Kristen Rose McGinnis, and Caroline Chick Jarrold\*



Cite This: J. Phys. Chem. A 2023, 127, 7264-7273



**Read Online** 

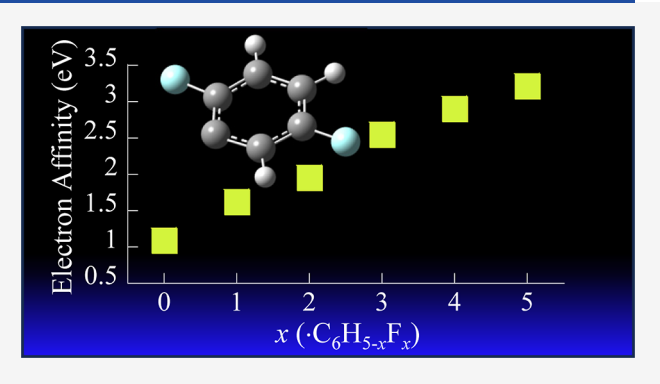
**ACCESS** 

III Metrics & More

Article Recommendations

Supporting Information

**ABSTRACT:** The electron affinities (EAs) of a series of  $C_6H_{5-x}F_x$  ( $1 \le x \le 4$ ) fluorophenyl radicals are determined from the photoelectron spectra of their associated fluorophenide anions generated from  $C_6H_{6-x}F_x$  ( $1 \le x \le 4$ ) fluorobenzene precursors. The spectra show a near-linear incremental increase in EA of 0.4 eV/x. The spectra exhibit vibrationally unresolved and broad detachment transitions consistent with significant differences in the molecular structures of the anion and neutral radical species. The experimental EAs and broad spectra are consistent with density functional theory calculations on these species. While the anion detachment transitions all involve an electron in a non-bonding orbital, the differences in structure between the neutral and anion are in part due to repulsion between the lone pair on the C-center on which the excess charge is



localized and neighboring F atoms. The  $C_6H_{5-x}F_x^-$  ( $2 \le x \le 4$ ) spectra show features at lower binding energy that appear to be due to constitutional isomers formed in the ion source.

# 1. INTRODUCTION

Benzene is of perspicuous central importance in organic chemistry. While it epitomizes stability associated with aromaticity, its electronic structure and chemistry can be strongly influenced by substituents. For example, methyl substitution decreases the ionization energy by enriching the electron density on the ring. Conversely, substituting with electron-withdrawing groups renders the ring electrophilic, driving the electron affinity (EA) of the closed shell neutral to be less negative, which can be tracked using electron transmission spectroscopy.  $^{1-6}$  Further increasing substitution with electron-withdrawing groups can result in positive EA. Indeed, in our own recent studies on fluorine-substituted benzenes, we determined the positive EA of pentafluorobenzene, which had previously been indirectly shown to be positive, in agreement with predictions by Driver and Jena. 9 Hexafluorobenzene was already known to have both a valencebound<sup>10-12</sup> and a correlation-bound<sup>13</sup> anion state.

In a related study on the photoelectron (PE) spectra of  $O_2^-$ .  $C_6H_{6-x}F_x$  ( $0 \le x \le 6$ ) complex anions, <sup>14</sup> we demonstrated a monotonic, but non-linear, increase in electron binding energy with x. Since the neutral  $O_2 \cdot C_6H_{6-x}F_x$  bimolecular complexes are all weakly bound by van der Waals interactions, the increase in binding energy of the anion was primarily the measure of the energy by which the  $O_2^-$  anion was stabilized by the neutral  $C_6H_{6-x}F_x$  partner (i.e., the solvent shift). Except for monofluorobenzene and pentafluorobenzene, which have only one structural isomer with modest dipole moments, the zero-dipole  $C_6H_{6-x}F_x$  structural isomers were used in the study

to avoid contributions from charge-dipole interactions in the  $O_2^- \cdot C_6 H_{6-x} F_x$  complex anion structures, allowing us to sample the intrinsic effects of the sequential fluorination of the benzene. While this evolution of electron binding energy with x can be taken in part as a measure of the impact of the electron withdrawal by the F atoms, a subsequent theoretical study on this series of complex anions showed that the situation was more complicated. Different structural isomers (e.g.,  $O_2^- \cdots H-C$  bonding versus  $O_2^- \cdots C$  interactions) have disparate charge delocalization from the  $O_2^-$  into the  $C_6 H_{6-x} F_x$  ring, and hence, the "solvent shift" observed in the spectrum is more nuanced. <sup>15</sup>

In this report, we present the PE spectra of a series of fluorinated phenide anions as an alternative approach toward achieving a quantitative measure of the impact of the electron-withdrawing groups on the electronic structure of this aromatic species. While  $C_6HF_5$  and  $C_6F_6$  are the only fluorinated benzenes that definitively form valence bound anions, the phenyl and substituted phenyl radicals,  $\cdot C_6H_{5-x}F_x$  are doublets and bind an electron to form a stable anion in a singlet state. Lineberger and co-workers demonstrated this using PE

Received: June 27, 2023 Revised: August 3, 2023 Published: August 21, 2023





spectroscopy on the  $C_6H_5^-$  phenide anion, <sup>16</sup> determining the EA of  $\cdot C_6H_5$  to be 1.096 eV. Anion PE spectroscopy has been an important tool used to explore the electronic structures of organic radical species, with several elegant examples included in refs 17–36. Of course, the phenyl radical in particular is an important intermediate in many chemical processes and has been the subject of numerous spectroscopic investigations, several of which are also included in refs 37–43.

As will be shown below, the EAs of the fluorophenyl radicals do indeed increase with increasing fluorination. To directly compare with the previous study on the detachment spectra of the  $O_2^{-}\cdot C_6H_xF_{6-x}$  complex anions, the fluorobenzenes selected for this study were monofluorobenzene, 1,4-difluorobenzene, 1,3,5-trifluorobenzene, and 1,2,4,5-tetrafluorobenzene. Of these four, only monofluorobenzene has a non-zero dipole moment. The pentafluorophenyl radical is not included in this study for practical reasons discussed below.

To further interpret the PE spectra, a series of calculations on the neutral radicals and their anions were completed, including on the different radical positions for the monofluorophenyl radical (the other species have only one possible structure, assuming no rearrangement of the F-atoms). We also calculated other structural isomers in which the benzene ring is not conserved, in an effort to explain features in several spectra that appeared to be electronic hot bands or higher energy structural isomers in the ion beam.

# 2. METHODS

**2.1. Experimental Details.** The substituted phenide anions were produced and spectroscopically probed using an anion PE imaging using an apparatus that has been described in detail elsewhere. Huorophenide ions were generated using a photoemission ion source in which a combination of low-energy electron production and photodissociation of a gas mixture composed of fluorobenzenes (seeded in an ultrahighpurity helium carrier gas) generated ions ranging from small carbon clusters to species with seven carbon atoms. As noted above, fluorobenzene (Sigma-Aldrich, 99% purity), 1,4-difluorobenzene (Sigma-Aldrich, 99% purity), 1,3,5-trifluorobenzene (97% purity), and 1,2,4,5-tetrafluorobenzene (Santa Cruz Biotechnology, 98% purity) were selected for this study.

The gas mixture was injected into the source using a pulsed molecular beam valve, operated at a 30 Hz repetition rate, flowing over a pressed  $Gd_2O_3$  powder target. The attenuated second harmonic output of a pulsed Nd:YAG laser (532 nm, 2.330 eV) was timed to irradiate the  $Gd_2O_3$  surface coincident with the gas pulse. The resulting anions were thermalized in a 10 mm long, 3 mm diameter channel before expanding into the vacuum chamber.

The gas mixture passed through a 2.5 mm skimmer, and the anions were accelerated to 1 kV into a 97 cm time-of-flight mass spectrometer, where species with different m/z separated in space and time. After passing through a mass defining slit, the ions collided with a dual microchannel plate ion detector. Drift times of the anions were recorded using a digitizing oscilloscope.

Prior to colliding with the ion detector, a packet of anions with a specific m/z were irradiated and photodetached with a second Nd:YAG laser. The PEs have kinetic energies that are related to the photon energy and the initial anion and final neutral states via

$$e^{-}KE = h\nu - EA - E_{int}^{neutral} + E_{int}^{anion}$$

where  $h\nu$  is the photon energy, EA is the neutral electron affinity,  $E_{\rm int}^{\rm neutral}$  represents the internal energy (electronic, vibrational, and rotational) of the neutral, and  $E_{\rm int}^{\rm anion}$  represents the same for the anion. If the anions are prepared with low internal energy, the e¯KE distribution largely reflects the energy levels of the neutral that are accessed by one-electron transitions.

The spectra presented below are plotted as a function of electron binding energy

$$e^{-}BE = h\nu - e^{-}KE$$

which is independent of photon energy, allowing for direct comparison of spectra obtained using different photon energies. The e<sup>-</sup>BE values directly represent the energy of the final neutral state relative to the initial state of the anion.

The photodetachment takes place at the intersection of the ion drift path and a velocity map imaging setup based on the design of Eppink and Parker  $^{46}$  and seminal work of Chandler and Houston.  $^{47}$  The resulting PEs are projected onto a 70 mm dual microchannel plate/phosphor screen assembly, and the resulting PE images were captured with a CCD camera, with the images saved using NuACQ 0.9 developed by the Suits group.  $^{48}$  The three-dimensional velocity distributions were extracted from the two-dimensional image using the BASEX program,  $^{49}$  and the resulting speed distribution was converted to electron kinetic energy (e^KE) by calibration against the well-known PE spectrum of  ${\rm O_2}^{-50}$ 

PE images were collected using both the second harmonic (532 nm, 2.330 eV) and third harmonic (355 nm, 3.4952 eV) outputs of a second Nd:YAG laser.

**2.2. Computational Details.** The molecular structures of the intact fluorophenyl neutral and fluorophenide anions that would be formed by a single C-H bond dissociation were optimized using B3LYP/aug-cc-pVTZ. The calculations were performed at the B3LYP level of theory, the results of which are readily comparable to calculations performed by Driver on various fluorobenzene molecules. It has been shown previously that the computationally expedient B3LYP functional is in good agreement with CCSD(T) for determining the EA of benzene.<sup>51</sup> Vibrational analysis was done to ensure that the structures were a local minimum. To compare directly with the anion PE spectra, the adiabatic EAs were calculated as the difference between the zero-point corrected energies of the optimized anions and neutrals. In addition, the vertical detachment energy (VDE), which is the binding energy at which the vibrational manifold of an electronic transition reaches maximum intensity, was calculated as the difference between the single-point calculated electronic energy of the neutral radical confined to the structure of the optimized anion and the electronic energy of the optimized anion.

All calculations were performed using the Gaussian 16 suites for electronic structure calculations. 52

Because the mass spectra showed evidence of varying degrees of fragmentation, we assumed that the intact fluorophenide species might be accompanied by other, less stable structures that could contribute to the anion PE spectra. Calculations on alternative constitutional isomers of the anions and neutrals were also conducted. These include fulvenyl- and Dewar-type structures as well as chain-like structures.

For a more detailed comparison between computed results and experimental spectra, spectral simulations based on computed structures, vibrational coordinates, vibrational frequencies, and relative energies were conducted using home written Labview codes, as described in detail previously.<sup>53</sup> We recently enhanced the code by making the extraction of the simulation parameters from the Gaussian output files more automated.

## 3. RESULTS AND ANALYSIS

**3.1. Mass Spectra.** Figure 1 shows a series of characteristic mass spectra of negative ions generated by  $C_6H_{6-x}F_x$  ( $1 \le x \le 4$ )-seeded helium flowing through the photoemission ion source as described in Section 2.1. The mass distribution is very sensitive to the laser fluence impinging on the  $Gd_2O_3$  target and how long the target has been in use. We, therefore,

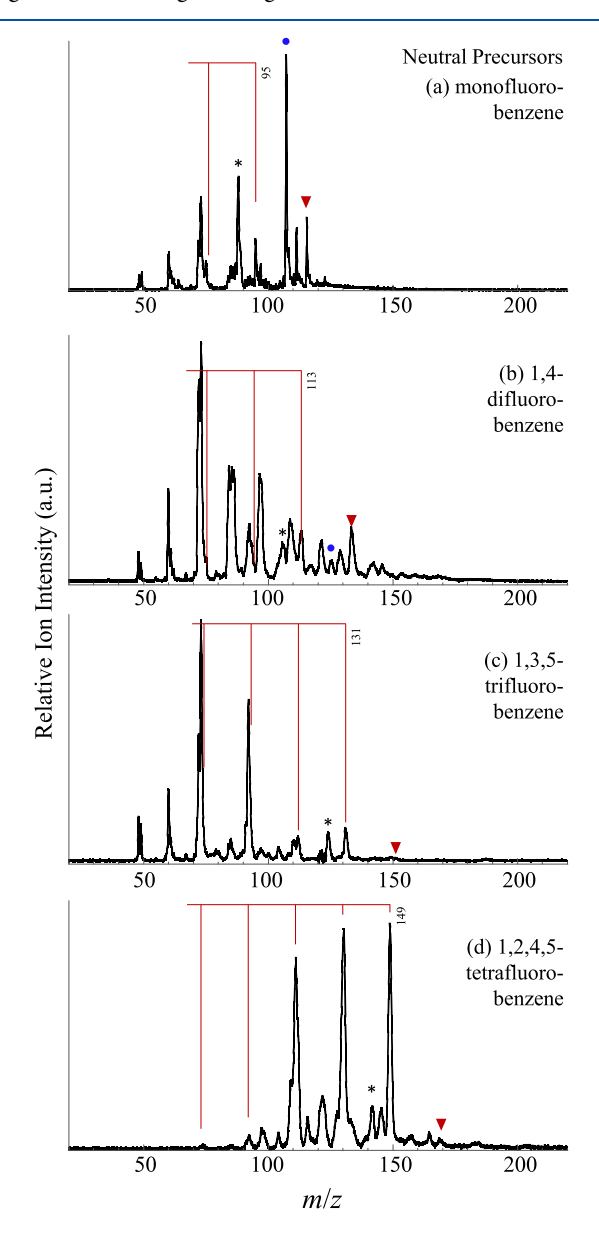


**Figure 1.** Mass spectra of negative ions generated from neutral (a) fluorobenzene, (b) 1,4-difluorobenzene, (c) 1,3,5-trifluorobenzene, and (d) 1,2,4,5-tetrafluorobenzene seeded in He carrier gas using the photoemission source described in Section 2.1. The m/z of the associated fluorophenides is included at the high m/z origin of the red combs, which guide the eye toward F-loss products from the fluorophenides. F $^-$ ·C<sub>6</sub>H<sub>6-x</sub>F<sub>x</sub> ions are indicated by red triangles, C-addition products are indicated by blue circles, and C-addition products with F-loss products are indicated by asterisks (\*).

provide a qualitative analysis of the source conditions necessary for production of the  $C_6H_{5-x}F_x^-$  ions based on these data.

As all molecules in the  $C_6H_{6-x}F_x$   $(1 \le x \le 3)$  series have been predicted to have negative EAs, <sup>9,15</sup> and as we previously demonstrated that the EA of C<sub>6</sub>H<sub>2</sub>F<sub>4</sub> is close to either zero or negative,7 we did not anticipate observing any intact  $C_6H_{6-x}F_x^-$  anions. Negative ions were produced only when higher laser fluence was used relative to the production of C<sub>6</sub>HF<sub>5</sub><sup>-</sup> and C<sub>6</sub>F<sub>6</sub><sup>-</sup>. As a result, significant fragmentation is evident for all four species. The red combs in Figure 1a through 1d show a series of m/z separated by 19, with the tine at the highest m/z (labeled with the m/z values) corresponding to the  $C_6H_{5-x}F_x^ (1 \le x \le 4)$  anion. Species observed at higher m/z can be attributed to  $F^-$ .  $C_6H_{6-x}F_x$ species (red triangle) or  $C_6H_{6-x}F_x$  that have undergone carbon atom addition (the subject of a subsequent report, blue circles). In most cases, we observe an anion with m/zconsistent with C-addition coupled with F- or HF-loss (asterisks). Several smaller carbon clusters or varyingly reduced carbon clusters  $(C_x H_y^-, x \ge 4, y \text{ depends on the precursor})$ molecule) are also observed with lower intensity. We note that the mass spectra shown are optimized for the mass ranges shown. F is also produced in very large quantities, and because of the high EA of F, it is very likely scavenging electrons in the source, another factor that makes generation of ions with lower EA challenging.

In the case of mono- and difluorobenzene (Figure 1a,b, respectively), the red combs indicating m/z consistent with F-loss fall to higher mass than the more intense ions near the comb tines in the mass spectra, suggesting HF loss as a potential dissociation channel. We note here that the 1,4-difluorobenzene sample required the highest laser fluences to generate anions, and more destructive processes are likely to be occurring.

These mass spectra serve to demonstrate that the production of these fluorophenides requires fairly destructive source conditions, but total atomization with subsequent re-formation of anionic species is not a major contributor to the anions observed. We, therefore, would anticipate  $C_6H_{5-x}F_x^-$  phenide structures that would be formed by simple C–H bond dissociation in the neutral  $C_6H_{6-x}F_x$  ( $1 \le x \le 4$ ) with subsequent electron attachment (or dissociation coupled with electron attachment) to form the closed shell fluorophenide anions.

Finally, we were unable to generate the pentafluorophenide anion in sufficient quantities, and fully spatially/temporally separated from the more abundant  $C_6HF_5^-$  anions using this source, to obtain a clean spectrum of this anion. The mass spectrum of ions generated using the source described above using pentafluorobenzene exhibited, in addition to  $C_6HF_5^-$ , several C-loss and F-loss species. A characteristic mass spectrum is included in the Supporting Information.

**3.2. PE Spectra of**  $C_6H_{5-x}F_x^-$  (1  $\leq x \leq$  4). Figure 2 shows the PE spectra of the  $C_6H_{5-x}F_x^-$  anions obtained using 3.495 eV photon energy (blue traces) and 2.330 eV photon energy (green traces). No signal rising above noise was observed in the spectrum of  $C_6H_4F^-$  using 2.330 eV photon energy, and in the case of  $C_6H_3F_2^-$ , the signal-to-noise ratio in the 2.330 eV is poor compared to the 2.330 eV spectra obtained for the more fluorinated species. Raw and transformed PE images are included in the Supporting Information.

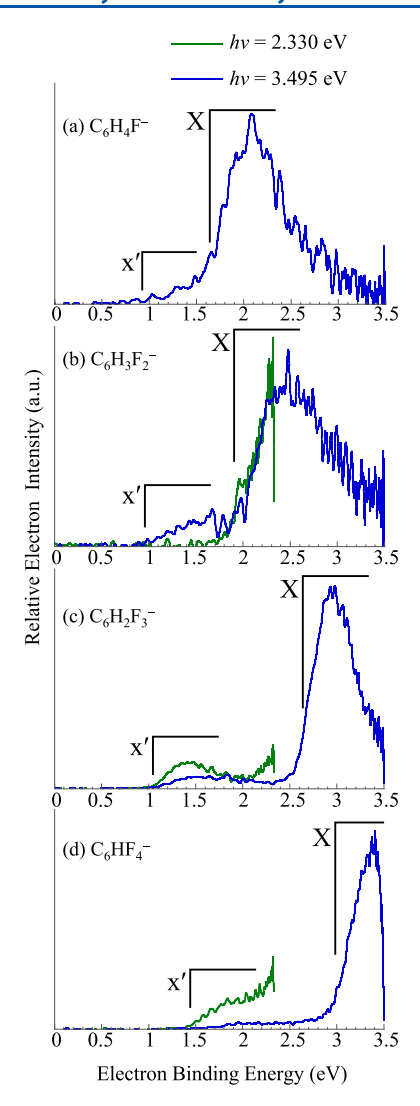


**Figure 2.** Anion PE spectra of (a)  $C_6H_4F^-$ , (b)  $C_6H_3F_2^-$ , (c)  $C_6H_2F_3^-$ , and (d)  $C_6HF_4^-$ , obtained using 3.495 eV (blue traces) and 2.33 eV (green traces).

The spectra obtained with 3.495 eV all exhibit an intense, broad transition labeled X. Identification of the spectral origin of band X in several cases is complicated by the appearance of a lower intensity feature at lower e^BE labeled x'. The PE spectra of  $C_6H_4F^-$  (Figure 2a) and  $C_6H_3F_2^-$  (Figure 2b) both appear to have partially resolved shoulders on the low-e^BE edge that are similar to the much better-resolved PE spectrum of phenide, <sup>16</sup> and the origins of band X shown in Figure 2 are consistent with the phenide vibrational manifold, though we assert a large margin of error. Based on these origins, the EA of  $\cdot C_6H_4F$  is  $1.63 \pm 0.15$  eV and the EA of  $\cdot C_6H_3F_2$  is  $1.96 \pm 0.15$  eV.

The PE spectra of  $C_6H_2F_3^-$  (Figure 2c) and  $C_6HF_4^-$  (Figure 2d) do not show distinct shoulders. Taking the position of 10% of the maximum intensity gives approximate EAs for the associated neutral radicals of 2.55  $\pm$  0.10 and 2.91  $\pm$  0.10 eV. The smaller errors are due to the steep rising edge of these vibrationally unresolved bands.

The primary experimental result is that each F-substitution on the phenyl radical results in an increase in EA of approximately 0.4 eV per F atom. The experimental ADEs

(which correspond to the neutral EA values) and VDEs are summarized in Table 1.

We now address the lower e<sup>-</sup>BE feature in several of the spectra. Except for the case of monofluorophenide (Figure 2a), the intensity of band x' relative to band X was inconsistent from day to day, suggesting the presence of the respective  $C_6H_{5-x}F_x^-$  anions in an excited state, or the presence of a higher energy constitutional isomer, in the ion beam. Control of the relative intensity of band x' was not clear-cut. Because of the low binding energy, with higher photoemission laser fluence (i.e., more violent source conditions), the species associated with band x' could be readily photodetached in the source as it was being produced. In addition, the surface of the photoemissive  $Gd_2O_3$  target evolved with usage. We rely on computations to help explain the source of band x' in the next section.

**3.3. Computational Results.** As pointed out by leading theoreticians, <sup>54</sup> organic radicals are "challenging systems to describe accurately". However, results presented below are in good agreement with the experimental results.

The extent of fragmentation in evidence in the mass spectra of ions generated experimentally calls into question whether the spectra represent species with an intact  $C_6$  aromatic ring. We, therefore, did calculations on all three possible isomers of  $C_6H_4F/C_6H_4F^-$ , along with all possible constitutional isomers of the other  $C_6H_{5-x}F_x$  and  $C_6H_{5-x}F_x^-$  (x=2,3,4) anions and neutrals, taking into account that the original zero-dipole structures might rearrange due to the high-energy ion source.

A summary of the computed energies of the singlet anions, the doublet neutrals, and the lowest energy triplet state of the anion is included in Table 1 for direct comparison with the experimental ADE and VDE values. Results on the phenyl radical and the phenide anion are included to demonstrate excellent agreement between the calculations and the vibrationally resolved PE spectrum of phenide reported by Lineberger and co-workers.<sup>16</sup>

First considering the monofluorophenyl radical, the calculations predict that all three structures of the neutral lie within a 0.1 eV window of energy, which suggests that the C—H bond dissociation energy is very similar for all three unique C—H bonds (o-, m-, and p- with respect to the C—F bond) with the 3-fluorophenyl (m-fluorophenyl) radical being the most stable. This result is consistent with the modestly deactivating effect of an electron-withdrawing substituent on a benzene molecule, which directs reactions toward the meta site. <sup>55</sup>

In contrast to results on the neutral, the 2-fluorophenide anion is favored more definitively over the 3- and 4-fluorophenide structures. The result of this greater separation between the three structures of the anion is that the most stable anion corresponds to the neutral with the highest EA. The computed ADE values, which correspond specifically to the lowest anion to lowest neutral states of each distinct structural isomer, correspond to the neutral EA values and range from 1.30 eV for the 4-fluorphenyl radical to 1.72 eV for the 2-fluorophenyl radical. Similarly, the VDE values range from 1.63 to 2.02 eV. Overall, the 2-fluorophenyl radical, which is computed to be the least stable of the three close-lying neutral isomers, and its corresponding anion, 2-fluorophenide, the lowest energy structure of the anion, give the best agreement with the experimental spectrum.

A simulation of the spectrum of 2-fluorophenide is shown in Figure 3 as the blue trace. While the profile of this simulation is

Table 1. Summary of Computed Zero-Point Corrected Energies, Adiabatic Detachment Energies, and Vertical Detachment Energies for the Fluorophenides and Corresponding Neutrals<sup>a</sup>

		computed energies (eV)			exp. (eV)
molecule		relative energy	ADE	VDE	ADE/VDE
phenyl	$^{2}$ A $_{1}$	1.06	1.06	1.40	1.096/1.36
phenide	$^{3}$ A	1.55			
	$^{1}A_{1}$	0			
2-fluorophenyl	$^{2}A'$	1.72	1.72	2.02	1.63/2.09
4-fluorophenyl	$^{2}A_{1}$	1.66	1.30	1.63	
3-fluorophenyl	$^{2}A'$	1.62	1.35	1.78	
			$(T_0)$		
4-fluorophenide	$^{3}A$	2.11	(1.75)		
	$^{1}A_{1}$	0.36			
3-fluorophenide	$^{3}A$	2.01	(1.74)		
	$^{1}A'$	0.27			
2-fluorophenide	$^{3}A$	2.19	(2.19)		
	$^{1}A'$	0			
2,5-difluorophenyl	$^{2}A'$	2.00	2.00	2.35	1.96/2.48
2,5-difluorophenide	$^{3}A$	2.32			
	$^{1}A'$	0			
2,4,6-trifluorophenyl	$^{2}A_{1}$	2.63	2.63	2.99	2.55/2.95
2,4,6-trifluorophenide	$^{3}A$	2.97			
	$^{1}A_{1}$	0			
1,2,4,5-tetrafluorophenyl	$^{2}A_{1}$	3.00	3.00	3.33	2.91/3.40
1,2,4,5-tetrafluorophenide	${}^{3}B_{1}$	3.22			
	$^{1}A_{1}$	0			
pentafluorophenyl	$^{2}A_{1}$	3.22	3.22	3.54	
pentafluorophenide	$^{3}A'$	2.71			
	$^{1}A_{1}$	0			

<sup>&</sup>lt;sup>a</sup>Note that only one structure for all of the species except for monofluorobenzene has only one possible position for the radical center, whereas monofluorobenzene has three. <sup>b</sup>Reference 16.

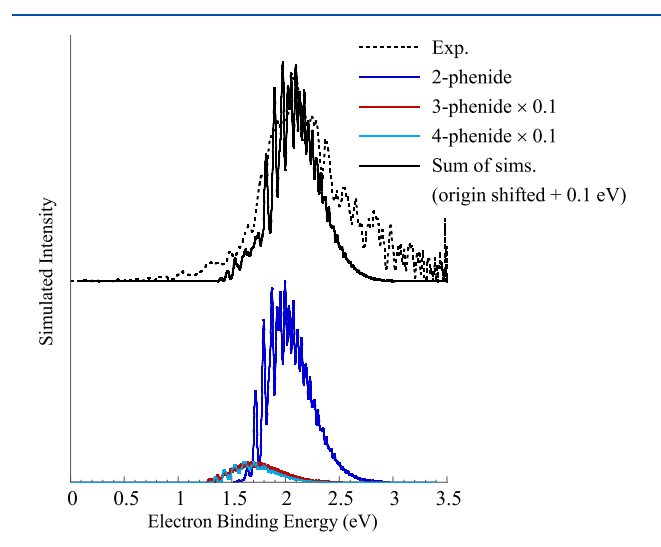


**Figure 3.** Computation-based simulations of the fluorophenide PE spectrum. Different colors are associated with the three different possible positions of the F to the radical center, with 2-phenide being computed to be the lowest energy. See text for more details on the relative intensities of the simulated spectra.

in good agreement with the experimental spectrum (dotted black trace), it does not capture the signal tailing to lower e<sup>-</sup>BE. However, this tail could be due to the presence of smaller abundances of the other isomers, whose spectra are shown as red and cyan traces. The maximum intensities of the

3- and 4-fluorophenide spectra are scaled to 0.1 of the 2-fluorophenide simulation maximum, though, as they are similar in position and profile, the scaling of each is somewhat arbitrary. Regardless, summing contributions from the higher energy anionic isomers with the 2-fluorophenide spectrum and shifting all origins by +0.09 eV (solid black trace) yield a simulation that is in consistent with the observed spectrum, without adjusting any other simulation parameters.

The fact that the three neutral radical structures are within 0.1 eV of each other but the most abundant anion corresponds to the least stable neutral suggests the following: all three neutrals can be formed during the photoemission laser pulse and all three can attach a low energy electron forming an anion that can then be thermalized by the helium buffer gas. However, the less stable anions can undergo H-shift, leading to the preferential formation of the 2-fluorophenide structure. The time between the production and detection of the anions is on the order of 300 microseconds, which is well under the half-life of radical ring 1,2 H migration. 56

In contrast to the monofluorophenide anion, the di-, tri-, and tetrafluorobenzene precursors targeted in this study have only one possible structural isomer for their respective fluorophenide anions, assuming no F-migration takes place. The computed ADE values all fall under 0.1 eV of the observed ADE values. The VDE values computed for 2,4,6-trifluorophenide (originating from 1,3,5-trifluorobenzene) and 2,3,5,6-tetrafluorophenide (originating from 1,2,4,5-trifluorobenzene) are within 0.07 eV of the experimental values. The

agreement in the case of 2,5-difluorophenide is less satisfactory, with the computed value being 0.13 eV below the observed value, but this disparity is not outside what can be considered reasonable. As noted above, higher laser fluences were required to produce ions from the 1,4-difluorobenzene sample, so hot bands and, potentially, other isomers might be populating the m/z 113 ion packet.

While F-migration would require longer timescale than Hmigration, we also calculated the ADE and VDE values for all the constitutional isomers of the  $C_6H_{5-x}F_x^-$  (2  $\leq x \leq 4$ ) molecules. These results are summarized in the Supporting Information. In the case of C<sub>6</sub>H<sub>3</sub>F<sub>2</sub><sup>-</sup>, the anion that would form directly from 1,4-difluorobenzene, 2,5-difluorophenide, is 0.31 eV above the most stable structure, 2,6-difluorophenide. The latter has a higher ADE and VDE than what is observed, suggesting that experimentally, F-rearrangement is not a significant factor. For the other two species, the ground-state structure of the anion is consistent with what would be formed by direct C-H bond dissociation and electron attachment, so question of rearrangement resulting in a lower energy anion is moot. A comparison of fluorophenides generated from different fluorobenzene precursor constitutional isomers will be the subject of a subsequent study.

While we were not able to isolate the pentafluorophenide anion experimentally from the neighboring and significantly more intense  $C_6HF_5^-$  ion, the computed detachment energy falls along the trendline for ADE and VDE values, suggesting that the spectrum would be similarly broad to the other spectra, shifted to higher e<sup>-</sup>BE relative to the tetrafluorophenide spectrum by 0.22 eV. The PE spectrum of the overlapping  $C_6F_5^-/C_6HF_5^-$  ion packet is included in the Supporting Information. The spectrum exhibits a signal with an origin of 3.22  $\pm$  0.05 eV, which may be attributed to  $C_6F_5^-$  based on the computed ADE, although it may also be attributed to the transition from the  $C_6HF_5^-$  anion to the triplet neutral state.<sup>7</sup>

Band  $\mathbf{x}'$  in the three more fluorinated species cannot be attributed to any constitutional isomers of each fluorophenide anion in which the benzene ring is conserved, and based on the fact that its appearance and relative intensity in the experimental spectrum are source condition-dependent, we consider the possibility of excited electronic states or higher energy constitutional isomers.

We first explore the possibility that the singlet anions might have a long-lived triplet state, which, upon photodetachment, would also access the ground doublet state of the neutral radical, but at lower e-BE values. The triplet states calculated for all  $C_6H_{5-x}F_x^-$  ( $1 \le x \le 4$ ) anions lie above the detachment continuum, and if formed in the ion source, would undergo autodetachment, eliminating the triplet states as a possible explanation. For example, the lowest energy triplet state of the o-fluorophenide anion is computed to be 2.19 eV, comparable to the D<sub>1</sub>-D<sub>0</sub> excitation energy of the neutral o-fluorophenyl radical of 2.01 eV<sup>57</sup> (and similar to other halophenyl radical excited-state energies  $^{58}$ ). This computed term energy is 0.47 eV above the neutral + free electron continuum. As a side note, the triplet state of pentafluorophenide is in contrast bound with respect to the detachment continuum, not because the triplet state is low-lying, but because the EA is higher than that of the other species.

We next consider the possibility that different structural isomers are populating the ion packet, such as the fluorinated fulvenide (5-methylene-1,3-cyclopentadienyl), dewar phenide

(bicyclo[2.2.0]hexa-2,5-dienide), and chain- or branched chain-like structures that have been suggested as intermediates in the gas-phase formation of benzene from smaller precursors. We focused on the tri-fluorinated isomers since band x' was most prevalent in the PE spectrum of  $C_6H_2F_3^-$ . Despite confining this search of constitutional isomers to the tri-fluorophenide, the potential structures formed by permuting the -H and -F atoms are numerous (see Supporting Information). However, the classes of different motifs (fulvenide, dewar-type, chains) group into different ranges of relative energies and ADEs.

The dewar tri-fluorophenide structures were found to be approximately 2 eV higher in energy than the lowest energy 2,4,6-trifluorophenide anion, and neutral radicals converged to the six-membered ring structures, meaning the detachment transitions would be very broad and at near-zero  $e^-BE$ , inconsistent with band  $\mathbf{x}'$ .

Eight tri-fluorofulvenide-type anion structures were computed to lie between 1.47 and 2.26 eV above the 2,4,6trifluorophenide anion. The associated fulvenyl neutrals were computed to have EAs ranging from 1.99 to 2.58 eV depending on the positions of the three F-centers and the position of the radical center. These values are inconsistent with the appearance of band x' at ca. 1.1 eV in the  $C_6H_2F_3^-$  PE spectrum. However, the anions are predicted to have low-lying triplet states, from which the ADE values range from 1.02 to 1.75 eV, again, depending on the specific structures. It is, therefore, possible that the band x' is due to excited states of isomers with the general fulvenide structure. If this is the case, band X would also have contributions from the detachment transition originating from the ground state of the fulvenide anion. The structures and relative energies of the fulvene-like structures are included in the Supporting Information.

Finally, numerous potential chain structures (e.g., 1,5-hexadiyni-3-yl with three F-substitutions) or branched chain structures (e.g., 2-ethynyl-1,3,butadiene-2-yl with three F-substitutions) were computed to lie over 2.7 eV and over 2.5 eV above the ground 2,4,6-trifluorophenide anion, respectively. The variability in the ADE values is wide for both classes of structures, ranging from 1.38 eV to over 3 eV. However, detachment transitions from the respective triplet states would again appear at lower e<sup>-</sup> BE. The Supporting Information includes diagrams showing the numerous singlet and triplet anions and doublet neutrals, along with their energies relative to the 2,4,6-trifluorophenide and 2,4,6-trifluorophenyl radicals.

While we cannot definitively assign band  $\mathbf{x}'$  to a specific structural isomer, calculations suggest that it is a kinetically trapped high-energy structure, possibly in an excited electronic state. While the relative intensity of band  $\mathbf{x}'$  to band  $\mathbf{X}$  did vary, the profile and  $\mathbf{e}^-\mathrm{BE}$  were consistent, suggesting that a specific kinetically favored species is being formed in the ion source.

## 4. DISCUSSION

Results presented in the previous section provide a firm relationship between the EAs of the  $\cdot C_6H_{5-x}F_x$  ( $1 \le x \le 4$ ) radical species with x for the series of radicals generated from the most symmetric fluorobenzene precursors. Figure 4a shows a plot of the experimentally ( $0 \le x \le 4$ , solid red boxes) and computationally ( $0 \le x \le 5$ , open red boxes) determined EAs of these radicals as a function of x (the EA of the phenyl radical determined by Lineberger and co-workers is included, as well as an EA potentially attributable to  $\cdot C_6F_5$  in the PE spectrum of  $C_6HF_5^{-}$ ). Circling back to an original motivation for this

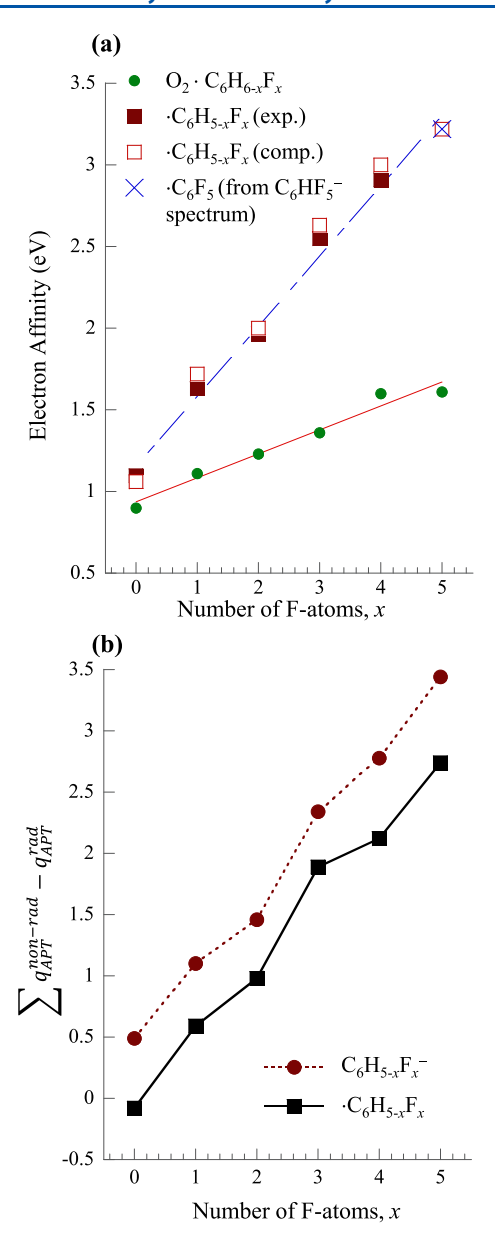


Figure 4. (a) Experimental (solid red squares) and computed (open red squares) EAs of the fluorophenyl radicals. The EA of the phenyl radical from ref 16 is included, along with the origin of signal that is attributed to pentafluorophenide (blue X) in the PE spectrum of  $C_6HF_5^-$  reported in ref 7. The green circles are the EAs of  $O_2^-$ ·  $C_6H_{6-x}F_x$  bimolecular complexes reported in ref 14. (b) Plot of the difference between the sum of the APT charges on the C atoms in the fluorobenzene backbone, excluding the radical center in the neutral or charge carrier in the anion, and the APT charge on the radical center (neutral, black squares), or the C atom carrying the excess charge (anion, red circles). More positive values indicate more extensive electron depletion of the carbon backbone, excluding the radical (or charged) center.

study, also included on the plot are the experimentally determined EAs of the  $O_2 \cdot C_6 H_{6-x} F_x$  van der Waals complexes, which change with increasing interaction between the  $O_2^-$  and the  $C_6 H_{6-x} F_x$  molecules with increasing x. It is clear from the plots that the EAs of the radicals and the EAs of the  $O_2 \cdot C_6 H_{6-x} F_x$  van der Waals complexes are not parallel, but they both show monotonic increases in EA with x. While grossly oversimplifying the analysis of these data, a linear regression of the experimental EA of the radicals versus x gives

a slope of 0.43 eV/x (R = 0.9958), while the van der Waals trend has a slope of 0.15 eV/x (R = 0.9848). Lines generated from the linear regressions of the EA values are included on the plot. The computed lowest energy structures of the  $O_2^-$ ·  $C_6H_{6-x}F_x$  complex anions (x < 6) are governed by the nonconventional C-H  $\cdots$   $O_2^-$  hydrogen bond, 60 which is strengthened as the H has an increasing partial positive charge with F-substitution. However, that effect is less dramatic (lower slope) than the dependence of electron binding energy of the anion of the corresponding radical species.

The significant increase in the EA of the  $\cdot C_6H_{6-x}F_x$  radicals is not manifested in the appearances of the highest occupied molecular orbital (HOMOs) of the respective anions, depictions of which are included in the Supporting Information. There is no obvious change in the spatial extent of the HOMO with binding energy. However, the experimental and computed EA values track with the charges on the C backbone. Figure 4b shows a plot of the difference between the sum of the APT charges on the fully bonded C centers and the APT charge on the radical C center in the neutral (black squares) or the C center carrying the charge in the anion (red circles). We will refer to this difference as the "charge disparity". The difference between the anionic and neutral charge disparities is less than one due to small changes in the APT charges on the other atoms in the  $C_6H_{5-x}F_x$  and C<sub>6</sub>H<sub>5-x</sub>F<sub>x</sub><sup>-</sup> species. The charge disparity trend, however, echoes the larger increase in EA from x = 0 and x = 1, as well as x = 2 to x = 3, when compared to the other increments. The slight deviation from a linear relationship between x and the charge disparity is likely due to more subtle symmetry effects, which is currently being explored in a study on the different isomers of the fluorobenzenes. However, the trend in EA with x clearly reflects the electron depletion in the C backbone of the fluorophenyl radicals. Of course, the individual APT charges on the backbone C atoms vary widely depending on whether the C-atom is bound to an F-atom, and the C-atom para to the radical center tends to be more negative/less positive than the ortho- and meta-C atoms with the same bonding partner (-H or -F; see Supporting Information). However, in a simple way, the radical EA is governed very directly by electrostatics.

We now consider the broad vibrational manifolds observed in the PE spectra. The HOMOs appear to be largely nonbonding, which is, at first glance, at odds with the vibrationally broadened PE spectra. There are no significant differences in the minor delocalization of the HOMO across the ring or adjacent C-F or C-H bonds, so no nuanced substituent placement effects appear to be at play. However, the neutral SOMOs (Supporting Information) are more delocalized over the full ring. The molecular structures of the anions and their associated neutrals, while all planar, have significant differences. The Supporting Information includes all structural parameters of the anions and neutrals. The primary differences lie in (1) the C-F bond length, which are predicted to be ca. 0.03 Å longer in the anion; (2) the  $C-[C\cdot]-C$  bond angle, which is significantly contracted in the anion. This appears to be the result of electrostatic repulsion between the localized electrons in the HOMO and adjacent F atoms; (3) the C-C bond lengths are different, with the  $[\cdot C]$ -C bond length longer in the anion, and then alternating shorter and longer C-C bond lengths. As a result of these three structural differences, many in-plane vibrational modes are excited in the detachment transition.

It is worth commenting on the mass spectra (Figure 1), all of which show a series of F-loss products, while the C<sub>6</sub> backbone appears to be largely conserved. The C-F bond dissociation energy in monofluorobenzene is higher than the C-H bond dissociation energy (532 kJ mol<sup>-1</sup> vs 466 kJ mol<sup>-1</sup>, respectively); however, we see that -F loss is more prevalent than -H loss.<sup>61</sup> While there is clear evidence of numerous destructive processes occurring in this ion source, we also note that the abundance of low kinetic energy electrons generated by the photoemitter are available to reduce the overall cost of C-F bond dissociation by the EA of F (3.401 eV) if F<sup>-</sup> ions are formed as a product. Indeed, temporary anion states of the neutral precursors may be involved in an overall dissociative attachment process leading to a defluorinated phenyl radical +F<sup>-,62</sup> with the radical subsequently undergoing electron attachment, as evidenced by the mass spectra.

We conclude this discussion by revisiting the relative stabilities of the three possible structures of the monofluor-ophenide anions. While the zero-dipole isomers of the more fluorinated species have only one possible isomer, the alternative isomers of di- and trifluorophenyl radicals (e.g., those formed from 1,2-difluorobenzene, 1,3-difluorobenzene, 1,2,3-trifluorobenzene, etc.) can support different radical isomers. A follow-up study on these different isomers is currently underway.

#### 5. CONCLUSIONS

The PE spectra of the fluorophenide anions are presented and compared to density functional theory calculations on the anions and their associated neutrals. The spectra of  $C_6H_{6-x}F_x^ (1 \le x \le 4)$  show a nearly linear increase in EA with x, in very good agreement with computed EAs of the radical species of structures formed by direct C–H bond dissociation in the formation of the radicals. The PE spectrum of the monofluorophenide anion is consistent with the lowest energy of three possible isomers computed for this anion. The isomers of the neutral fluorophenyl radical are very close in energy, suggesting that if C–H bond dissociation precedes electron attachment, the resulting anion may undergo H-shift to form the most stable anionic structure.

Calculations on the fluorophenide anions and neutrals predict planar structures, but with significant differences between the anions and neutrals, which is consistent with the vibrationally broadened spectra. Despite the substantial increase in the EAs of the  $\cdot C_6H_{6-x}F_x$  radicals with x, the calculations predict nearly identical HOMOs across the series. The change in EA is, therefore, evidently related mainly to the electron-depletion of the  $C_6$  ring, rather than any more nuanced effects associated with the position of the F-substitutions on the  $C_6$  ring.

# ASSOCIATED CONTENT

# Supporting Information

The Supporting Information is available free of charge at https://pubs.acs.org/doi/10.1021/acs.jpca.3c04327.

Raw and reconstructed photoelectron images, mass spectrum of anions generated from pentafluorobenzene seeded in He via the photoemission source, PE spectrum of  $C_6HF_5^-$  from ref 7, full structural parameters for  $C_6H_{6-x}F_x^-$  and  $\cdot C_6H_{6-x}F_x$  (x=1-4), computation results on different constitutions isomers of the  $\cdot C_6H_{6-x}F_x$  radicals and their anions, and diagrams

showing the relative energies of different structural isomers in which the  $C_6$  ring is not conserved (PDF)

## AUTHOR INFORMATION

## **Corresponding Author**

Caroline Chick Jarrold — Department of Chemistry, Indiana University, Bloomington, Indiana 47405, United States; orcid.org/0000-0001-9725-4581; Email: cjarrold@indiana.edu

#### **Authors**

Conor J. McGee – Department of Chemistry, Indiana University, Bloomington, Indiana 47405, United States Kristen Rose McGinnis – Department of Chemistry, Indiana University, Bloomington, Indiana 47405, United States

Complete contact information is available at: https://pubs.acs.org/10.1021/acs.jpca.3c04327

#### Notes

The authors declare no competing financial interest.

#### ACKNOWLEDGMENTS

This material is based upon work supported by the National Science Foundation under grant no. 2053889.

### REFERENCES

- (1) Jordan, K. D.; Burrow, P. D. Temporary anion states of polyatomic hydrocarbons. *Chem. Rev.* 1987, 87, 557–588.
- (2) Burrow, P. D.; Michejda, J. A.; Jordan, K. D. Electron Transmission Study of the Temporary Negative Ion States of Selected Benzenoid and Conjugated Aromatic Hydrocarbons. *J. Chem. Phys.* 1987, 86, 9–24.
- (3) Venuti, M.; Modelli, A. Low-Energy Electron Attachment to Fused 1,4-Cyclohexadiene Rings by Means of Electron Transmission Spectroscopy and Exponent Stabilization Calculations. *J. Chem. Phys.* **2000**, *113*, 2159–2167.
- (4) Pshenichnyuk, S. A.; Modelli, A. Electron Attachment to Antipyretics: Possible Implications of their Metabolic Pathways. *J. Chem. Phys.* **2012**, *136*, 234307.
- (5) Modelli, A.; Jones, D. Temporary Anion States and Dissociative Electron Attachment to Isothiocyanates. *J. Phys. Chem. A* **2006**, *110*, 13195–13201.
- (6) Csonka, I. P.; Szepes, L.; Modelli, A. Donor–Acceptor Properties of Isonitriles Studied by Photoelectron Spectroscopy and Electron Transmission Spectroscopy. *J. Mass Spectrom.* **2004**, *39*, 1456–1466.
- (7) McGee, C. J.; McGinnis, K. R.; Jarrold, C. C. Anion Photoelectron Imaging Spectroscopy of  $C_6HF_5^-$ ,  $C_6F_6^-$ , and the Absence of  $C_6H_2F_4^-$ . Submitted to *J. Chem. Phys. A* **2023**.
- (8) Wentworth, W. E.; Limero, T.; Chen, E. C. M. Electron Affinities of Hexafluorobenzene and Pentafluorobenzene. *J. Phys. Chem.* **1987**, 91, 241–245.
- (9) Driver, N.; Jena, P. Electron Affinity of Modified Benzene. *Int. J. Quantum Chem.* **2017**, *118*, No. e25504.
- (10) Eustis, S. N.; Wang, D.; Bowen, K. H.; Naresh Patwari, G. Photoelectron Spectroscopy of Hydrated Hexafluorobenzene Anions. *J. Chem. Phys.* **2007**, *127*, 114312.
- (11) Rogers, J. P.; Anstöter, C. S.; Bull, J. N.; Curchod, B. F. E.; Verlet, J. R. R. Photoelectron Spectroscopy of the Hexafluorobenzene Cluster Anions:  $(C_6F_6)_n$  (n = 1–5) and I ( $C_6F_6$ ). *J. Phys. Chem. A* **2019**, 123, 1602–1612.
- (12) Nakajima, A.; Taguwa, T.; Hoshino, K.; Sugioka, T.; Naganuma, T.; Oho, F.; Watanabe, K.; Nakao, K.; Konishi, Y.; Kishi, R.; et al. Photoelectron spectroscopy of  $(C_6F_6)_n^-$  and  $(Au-C_6F_6)^-$  clusters. *Chem. Phys. Lett.* **1993**, 214, 22–26.

- (13) Voora, V. K.; Jordan, K. D. Nonvalence Correlation-Bound Anion State of C<sub>6</sub>F<sub>6</sub>: Doorway to Low-Energy Electron Capture. *J. Phys. Chem. A* **2014**, *118*, 7201–7205.
- (14) Dobulis, M. A.; Thompson, M. C.; Sommerfeld, T.; Jarrold, C. C. Temporary anion states of fluorine substituted benzenes probed by charge transfer in  $O_2^- \cdot C_6 H_{6-x} F_x$  (x = 0-5) ion-molecule complexes. *J. Chem. Phys.* **2020**, *152*, 204309.
- (15) Davis, J. U.; Jarrold, C. C.; Sommerfeld, T. Charge Distribution in Oxygen-Fluorobenzene Complex Anions  $[O_2 \cdot C_6 H_{6-n} F_n]^-$  (n = 0 6). Chem. Phys. 2023, 574, 112023.
- (16) Gunion, R. F.; Gilles, M. K.; Polak, M. L.; Lineberger, W. C. Ultraviolet Photoelectron Spectroscopy of the Phenide, Benzyl and Phenoxide anions, with ab initio Calculations. *Int. J. Mass Spectrom. Ion Processes* **1992**, *117*, 601–620.
- (17) Wenthold, P. G.; Squires, R. R.; Lineberger, W. C. Ultraviolet Photoelectron Spectroscopy of the *o-m-*and *p-*Benzyne Negative Ions. Electron Affinities and Singlet-Triplet Splittings for *o-m-*and *p-*Benzyne. *J. Am. Chem. Soc.* **1998**, *120*, 5279–5290.
- (18) Gibbard, J. A.; Continetti, R. E. Photoelectron Photofragment Coincidence Spectroscopy of Carboxylates. *RSC Adv.* **2021**, *11*, 34250–34261.
- (19) Gibbard, J. A.; Castracane, E.; Shin, A. J.; Continetti, R. E. Dissociative Photodetachment Dynamics of the Oxalate Monoanion. *Phys. Chem. Chem. Phys.* **2020**, 22, 1427–1436.
- (20) Lunny, K. G.; Benitez, Y.; Albeck, Y.; Strasser, D.; Stanton, J. F.; Continetti, R. E. Spectroscopy of Ethylenedione and Ethynediolide: A Reinvestigation. *Angew. Chem., Int. Ed.* **2018**, *57*, 5394–5397.
- (21) Benitez, Y.; Nguyen, T. L.; Parsons, A. J.; Stanton, J. F.; Continetti, R. E. Probing the Exit Channel of the OH + CH<sub>3</sub>OH  $\rightarrow$  H<sub>2</sub>O + CH<sub>3</sub>O Reaction by Photodetachment of CH<sub>3</sub>O<sup>-</sup>(H<sub>2</sub>O). *J. Phys. Chem. Lett.* **2022**, *13*, 142–148.
- (22) Schwartz, R. L.; Davico, G. E.; Ramond, T. M.; Lineberger, W. C. Singlet-Triplet Splittings in CX<sub>2</sub> (X = F, Cl Br, I) Dihalocarbenes via Negative Ion Photoelectron Spectroscopy. *J. Phys. Chem. A* **1999**, 103, 8213–8221.
- (23) Bouwman, J.; Hrodmarsson, H. R.; Ellison, G. B.; Bodi, A.; Hemberger, P. Five Birds with One Stone: Photoelectron Photoion Coincidence Unveils Rich Phthalide Pyrolysis Chemistry. *J. Phys. Chem. A* **2021**, *125*, 1738–1746.
- (24) Culberson, L. M.; Blackstone, C. C.; Wallace, A. A.; Sanov, A. Aromatic Stabilization and Hybridization Trends in Photoelectron Imaging of Heterocyclic Radicals and Anions. *J. Phys. Chem. A* **2015**, 119, 9770–9777.
- (25) Wallace, A. A.; Dauletyarov, Y.; Sanov, A. Diradical Interactions in Ring-Open Isoxazole. *J. Phys. Chem. A* **2021**, *125*, 317–326.
- (26) Laws, B. A.; Levey, Z. D.; Sanov, A.; Stanton, J. F.; Schmidt, T. W.; Gibson, S. T. Velocity Map Imaging Spectroscopy of  $C_2H^-$  and  $C_2D^-$ : A Benchmark Study of Vibronic Coupling Interactions. *J. Chem. Phys.* **2022**, *157*, 044305.
- (27) Dixon, A. R.; Khuseynov, D.; Sanov, A. Heterogeneously Substituted Radicals and Carbenes: Photoelectron Imaging of the FC(H)CN<sup>-</sup> and FCCN<sup>-</sup> Anions. *J. Phys. Chem. A* **2014**, *118*, 8533–8541.
- (28) Anstöter, C. S.; Rogers, J. P.; Verlet, J. R. Spectroscopic Determination of an Anion- $\pi$  Bond Strength. *J. Am. Chem. Soc.* **2019**, 141. 6132–6135.
- (29) Hossain, E.; Deng, S. M.; Gozem, S.; Krylov, A. I.; Wang, X. B.; Wenthold, P. G. Photoelectron Spectroscopy Study of Quinonimides. *J. Am. Chem. Soc.* **2017**, *139*, 11138–11148.
- (30) Lau, J. A.; DeWitt, M.; Boyer, M. A.; Babin, M. C.; Solomis, T.; Grellmann, M.; Asmis, K. R.; McCoy, A. B.; Neumark, D. M. High-Resolution Photoelectron Spectroscopy of Vibrationally Excited Vinoxide Anions. *J. Phys. Chem. A* **2023**, *127*, 3133–3147.
- (31) DeWitt, M.; Babin, M. C.; Lau, J. A.; Solomis, T.; Neumark, D. M. High Resolution Photoelectron Spectroscopy of the Acetyl Anion. *J. Phys. Chem. A* **2022**, *126*, 7962–7970.
- (32) DeVine, J. A.; Babin, M. C.; Blackford, K.; Neumark, D. M. High-Resolution Photoelectron Spectroscopy of the Pyridinide Isomers. *J. Chem. Phys.* **2019**, *151*, 064302.

- (33) Harrison, A. W.; Ryazanov, M.; Sullivan, E. N.; Neumark, D. M. Photodissociation Dynamics of the Methyl Perthiyl Radical at 248 and 193 nm using Fast-Beam Photofragment Translational Spectroscopy. *J. Chem. Phys.* **2016**, *145*, 024305.
- (34) Neumark, D. M. Spectroscopy of Radicals, Clusters, and Transition States Using Slow Electron Velocity Map Imaging of Cryogenically Cooled Anions. *J. Phys. Chem. A* **2023**, 127, 4207–4223.
- (35) Stokes, S. T.; Bartmess, J. E.; Buonaugurio, A.; Wang, Y.; Eustis, S. N.; Bowen, K. H. Anion Photoelectron Spectroscopy of the Linear  $C_nH_{2h+1}O^-$  (n = 1-9) Alkoxides. *Chem. Phys. Lett.* **2019**, 732, 136638.
- (36) Patros, K. M.; Mann, J. E.; Dobulis, M. A.; Thompson, M. C.; Jarrold, C. C. Probing Alkenoxy Radical Electronic Structure using Anion PEI Spectroscopy. *J. Chem. Phys.* **2019**, *150*, 034302.
- (37) Radziszewski, J. G.; Nimlos, M. R.; Winter, P. R.; Ellison, G. B. Infrared Absorption Spectroscopy of the Phenyl Radical. *J. Am. Chem. Soc.* **1996**, *118*, 7400–7401.
- (38) Friderichsen, A. V.; Radziszewski, J. G.; Nimlos, M. R.; Winter, P. R.; Dayton, D. C.; David, D. E.; Ellison, G. B. The Infrared Spectrum of the Matrix-Isolated Phenyl Radical. *J. Am. Chem. Soc.* **2001**, *123*, 1977–1988.
- (39) Chang, C.-H.; Nesbitt, D. J. High Resolution Spectroscopy of Jet Cooled Phenyl Radical: The v<sub>1</sub> and v<sub>2</sub> a<sub>1</sub> Symmetry C–H Stretching Modes. *J. Chem. Phys.* **2016**, *145*, 044304.
- (40) Sharp, E. N.; Roberts, M. A.; Nesbitt, D. J. Rotationally Resolved Infrared Spectroscopy of a Jet-Cooled Phenyl Radical in the Gas Phase. *Phys. Chem. Chem. Phys.* **2008**, *10*, 6592–6596.
- (41) Freel, K.; Park, J.; Lin, M. C.; Heaven, M. C. Cavity ring-down spectroscopy of the phenyl radical in a pulsed discharge supersonic jet expansion. *Chem. Phys. Lett.* **2011**, *507*, 216–220.
- (42) Radziszewski, J. G. Electronic Absorption Spectrum of Phenyl Radical. *Chem. Phys. Lett.* **1999**, *301*, 565–570.
- (43) Cole-Filipiak, N. C.; Shapero, M.; Negru, B.; Neumark, D. M. Revisiting the Photodissociation Dynamics of the Phenyl Radical. *J. Chem. Phys.* **2014**, *141*, 104307.
- (44) Williams, B. A.; Siedle, A. R.; Jarrold, C. C. Identification of Stable Perfluorocarbons Formed by Hyperthermal Decomposition of Graphite Fluoride Using Anion Photoelectron Spectroscopy. *J. Phys. Chem. C* **2022**, *126*, 9965–9978.
- (45) Mann, J. E.; Troyer, M. E.; Jarrold, C. C. Photoelectron Imaging and Photodissociation of Ozonide in  $O_3^- \cdot (O_2)_n$  (n = 1 4). *J. Chem. Phys.* **2015**, *142*, 124305.
- (46) Eppink, A. T. J. B.; Parker, D. H. Velocity Map Imaging of Ions and Electrons using Electrostatic Lenses: Application in Photoelectron and Photofragment Ion Imaging of Molecular Oxygen. *Rev. Sci. Instrum.* 1997, 68, 3477–3484.
- (47) Chandler, D. W.; Houston, P. L. Two-Dimensional Imaging of State-Selected Photodissociation Products Detected by Multiphoton Ionization. *J. Chem. Phys.* **1987**, *87*, 1445–1447.
- (48) Doyle, M. B.; Abeyasera, C.; Suits, A. G. NuAcq 0.9: Native Megapixel Ion Imaging with Centroiding to 4 Mpix Using Inexpensive USB-2 Cameras. 2020, Available at http://faculty.missouri.edu/suitsa/NuAqc.html (accessed Feb 4, 2020).
- (49) Dribinski, V.; Ossadtchi, A.; Mandelshtam, V. A.; Reisler, H. Reconstruction of Abel-Transformable Images: The Gaussian Basis-Set Expansion Abel Transform Method. *Rev. Sci. Instrum.* **2002**, *73*, 2634–2642.
- (50) Ervin, K. M.; Anusiewicz, I.; Skurski, P.; Simons, J.; Lineberger, W. C. The Only Stable State of  ${\rm O_2}^-$  is the X  $^2\Pi_{\rm g}$  Ground State and it (Still!) Has an Adiabatic Electron Detachment Energy of 0.45 eV. *J. Phys. Chem. A* **2003**, *107*, 8521–8529.
- (51) Hajgató, B.; Deleuze, M. S.; Tozer, D. J.; De Proft, F. A Benchmark Theoretical Study of the Electron Affinities of Benzene and Linear Acenes. *J. Chem. Phys.* **2008**, *129*, 084308.
- (52) Firsch, M. J.; Trucks, G. W.; Schlegel, H. B.; Scuseria, G. E.; Robb, M. A.; Cheeseman, J. R.; Scalmani, G.; Barone, V.; Mennucci, B.; Petersson, G. A.; et al. *Gaussian 16*; Gaussian Inc.: Wallingford, CT, USA, 2016.

- (53) Schaugaard, R. N.; Topolski, J. E.; Ray, M.; Raghavachari, K.; Jarrold, C. C. Insight into Ethylene Interactions with Molybdenum Suboxide Cluster Anions from Photoelectron Spectra of Chemifragments. J. Chem. Phys. 2018, 148, 054308.
- (54) Sadhukhan, T.; Beckett, D.; Thapa, B.; Raghavachari, K. Coupling Constants, High Spin, and Broken Symmetry States of Organic Radicals: an Assessment of the Molecules-in-Molecules Fragmentation-Based Method. *J. Chem. Theory Comput.* **2019**, *15*, 5998–6009.
- (55) Ege, S. Organic Chemistry; D.C. Heath and Company: Lexington, Mass. 1984.
- (56) Pezacki, J. P.; Couture, P.; Dunn, J. A.; Warkentin, J.; Wood, P. D.; Lusztyk, J.; Ford, F.; Platz, M. S. Rate Constants for 1,2-Hydrogen Migration in Cyclohexylidene and in Substituted Cyclohexylidenes. *J. Org. Chem.* 1999, 64, 4456–4464.
- (57) Leugers, M. A.; Gill, R. J.; Atkinson, G.H. o-Fluorophenyl Radical: Analysis of the  $n \leftarrow \pi$  Vibronic Spectrum and the Formation Kinetics in o-Fluorobromobenzene Photolysis. *Chem. Phys. Lett.* **1983**, 94, 393–397.
- (58) Porter, G.; Ward, B. The Electronic Spectra of Phenyl Radicals. *Proc. R. Soc. London, A* **1965**, 287, 457–470.
- (59) Zhao, L.; Lu, W.; Ahmed, M.; Zagidullin, M. V.; Azyazov, V. N.; Morozov, A. N.; Mebel, A. M.; Kaiser, R. I. Gas-Phase Synthesis of Benzene via the Propargyl Radical Self-Reaction. *Sci. Adv.* **2021**, *7*, No. eabf0360.
- (60) Gu, Y.; Kar, T.; Scheiner, S. Fundamental Properties of the CH···O Interaction: Is It a True Hydrogen Bond? *J. Am. Chem. Soc.* 1999, 121, 9411–9422.
- (61) Rumble, J. R.; Bruno, T. J.; Doa, M. J. CRC Handbook of Chemistry and Physics: A Ready-Reference Book of Chemical and Physical Data; Crc Press/Taylor & Francis Group: Boca Raton, 2022.
- (62) Massey, H. S. W. Dissociative Attachment; Endeavor, 1980; Vol. 4, pp 78–84.